

Influence of mixing conditions on rheological behavior and electrical conductivity of polyamides filled with carbon black

Mathilde Leboeuf · Nessim Ghamri · Benoît Brulé ·
Thierry Coupez · Bruno Vergnes

Received: 11 April 2007 / Accepted: 20 October 2007 / Published online: 12 November 2007
© Springer-Verlag 2007

Abstract The introduction of carbon black in a polyamide matrix allows one to obtain conductive materials because of the formation of a filler network. Resulting electrical properties depend, among others, on the processing conditions. In a first part, we investigate the influence of mixing conditions (rotor speed, temperature, mixing time) on electrical conductivity. Then, in a second part, we try to characterize the conducting network by rheological measurements and to establish relationships between rheological parameters and electrical properties. For that purpose, we propose to perform successive strain sweep experiments at constant frequency, from 0.5 to 100%, then from 100 to 0.5%, and finally, again, from 0.5 to 100%. Between two successive strain sweeps, we observe a drop in the moduli values that can be attributed to the breakdown of the carbon black network. A clear relationship is established between rheological and electrical properties of the compounds. Moreover, we propose a presentation of the rheological data that permits to rank the samples according to the strength of the carbon black network.

Keywords Polyamide · Carbon black · Electrical resistivity · Network · Structure breakdown

Introduction

It is well known for a long time that the introduction of carbon black (CB) in a polymer matrix allows one to obtain conductive materials with low resistivity (Sichel 1982; Margolis 1989). The electrical resistivity decreases when CB content increases because of the formation of a conductive network throughout the isolating matrix (Medalia 1986). Different models of percolation may describe these effects (Lux 1993a,b). When the CB concentration increases, the distance between particles decreases, thus, facilitating the transport of electrons and reducing the electrical resistivity (Khojjiya et al. 2005). The properties of the conductive polymer composites (CPC) depend not only on the quantity of CB, its characteristics (Boonstra and Medalia 1963), and the characteristics of the matrix (molecular weight, crystallinity), but also on the level of filler dispersion (Yu et al. 2005), resulting, among others, from the mixing conditions (Das et al. 2002; Feller et al. 2002, Feller and Petitjean 2003). The objectives of the present work are, thus, to optimize the processing conditions to obtain a required level of resistivity with a minimum value of CB content. Indeed, a reduction in filler content is beneficial for the mechanical properties required for the targeted application of these materials.

However, a difficulty in the study of CB-filled polymers is that, at high filler content, the observation of the percolated network by techniques of electronic microscopy remains difficult, even if recent techniques based on atomic force microscopy (AFM; Ravier et al. 2001; Carmona and Ravier 2002) or 3D transmission electron microscopy (TEM; Kohjiya et al. 2005, 2006) appears promising. Therefore, alternative techniques, such as rheometry, have been developed. For example, Bar-Chaput and Carrot (2006) characterized CB dispersion in a polyethylene oxide

M. Leboeuf · T. Coupez · B. Vergnes (✉)
Cemef, Ecole des Mines de Paris, UMR CNRS 7635,
BP 207,
06904 Sophia-Antipolis Cedex, France
e-mail: bruno.vergnes@ensmp.fr

M. Leboeuf · N. Ghamri · B. Brulé
Cerdato, Arkema,
27470 Serquigny, France

matrix by small amplitude oscillatory shear measurements. They established a correlation between the increase of storage modulus at low frequency and the state of dispersion. Wu et al. (2000, 2006) and Wu and Zheng 2004 put in evidence a relationship between electrical and viscoelastic percolations. Viscoelastic percolation is characterized by a sharp variation of the ratio of storage modulus of CPC and matrix (at low frequency) when increasing CB content.

In the present work, we will first characterize the influence of mixing conditions (rotor speed, temperature, mixing time) on the electrical properties of polyamide/CB CPC. Then, we will study the rheological behavior of compounds with different CB content prepared in the same mixing conditions, and we will establish relationships between electrical and rheological properties. Finally, we will compare the results obtained with different mixing conditions to define the most favorable conditions.

Materials and methods

Materials

The polymer matrix used in this study is not a pure polyamide but a blend of polyamide 12 (PA12 Rilsan© A, Arkema, France) and polyether block amide (Pebax© 33, Arkema, France). Pebax© is added to reinforce the impact properties of PA12. Of course, the use of a blend leads to more complexity. It is well known that, in this case, the morphology of the matrix may play an important role (Pötschke et al. 2003, 2004; Yui et al. 2006). CB can be dispersed in one phase, in both, or selectively located at the interfaces. The concept of double percolation (Thongruang et al. 2002; Pötschke et al. 2004; Meincke et al. 2004) implies that conductivity of the material is obtained when CB percolates across a phase that itself percolates across the matrix. However, in our case, things are different, and this aspect of the problem can be disregarded at first approximation. First of all, Pebax© concentration is low and the ratio Pebax©/PA12 is maintained constant for all the experiments (for confidential reasons, we are not allowed to provide the value of Pebax© concentration, but it remains lower than 20 wt%). Consequently, Pebax© always appears as a nodular phase dispersed in the continuous PA12 matrix. This is clearly shown in Fig. 1a for a compound with 17 wt% CB (TEM, Philips CM12 with an accelerating voltage of 120 kV). The white nodules are Pebax© when the gray continuous phase is made of PA. Nodule size is heterogeneous and varies between 0.25 and 3 μm . At higher magnification (Fig. 1b and c), we may observe CB aggregates of about 100 nm, more or less organized as strings. The second important point is that CB

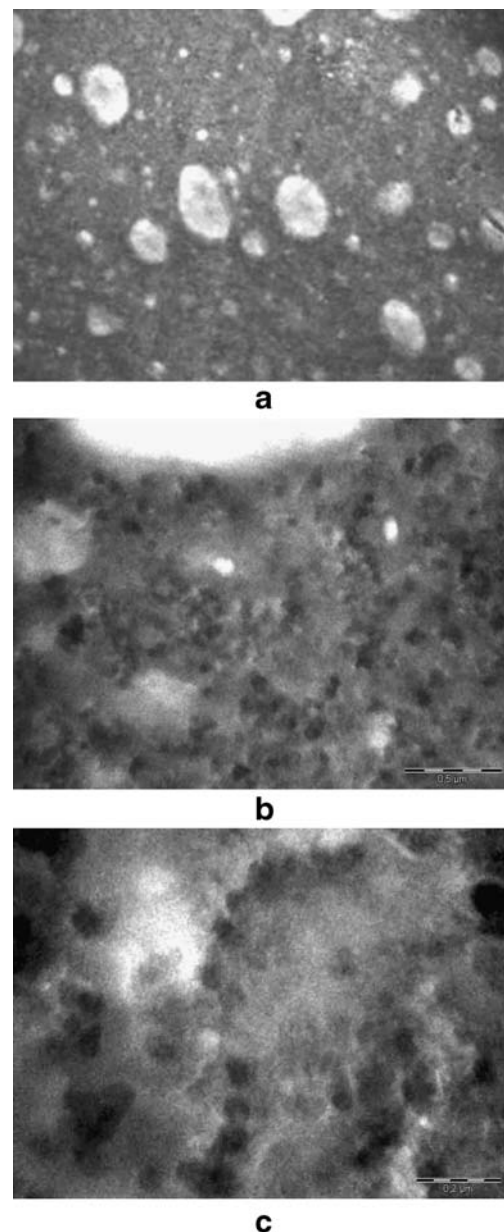
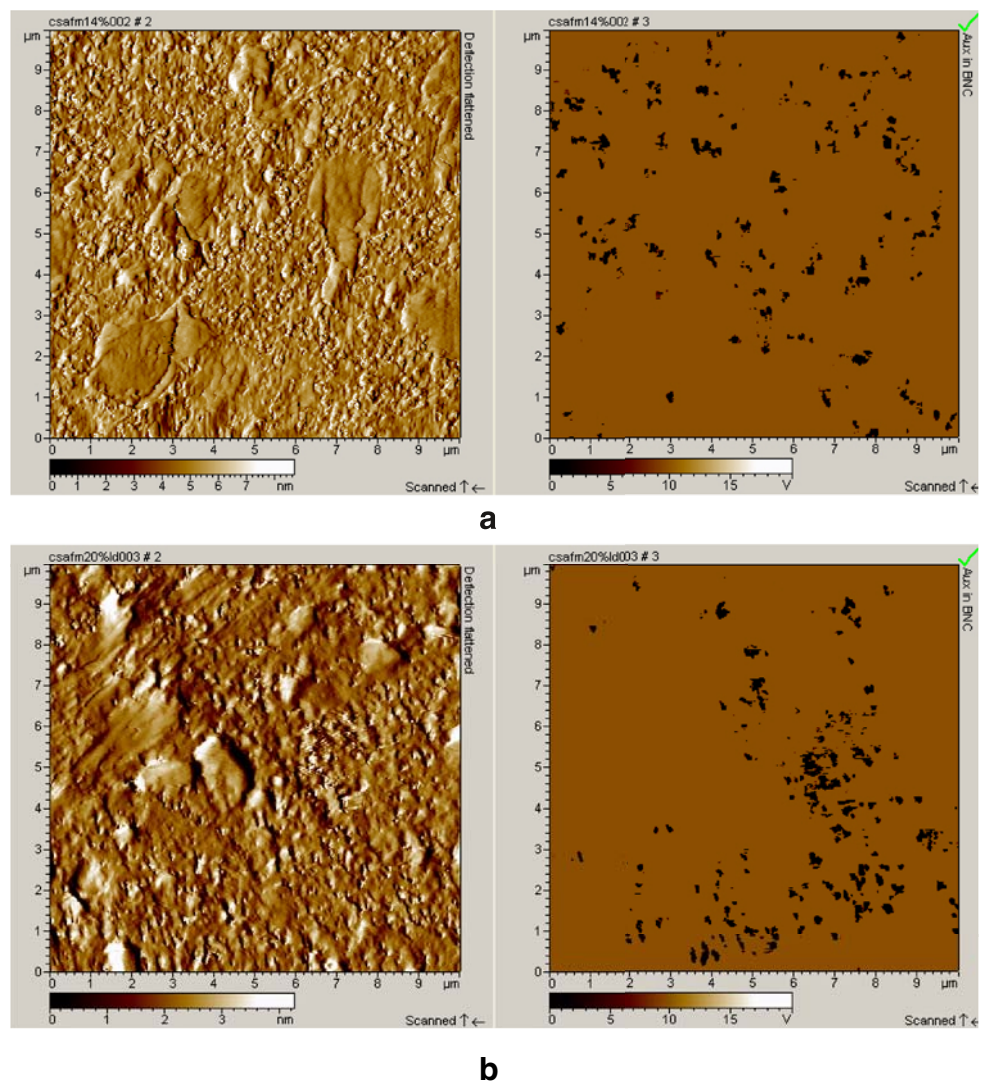


Fig. 1 TEM images of a compound with 17 wt% CB (240 °C, 50 rpm, 4 min). **a** Magnification 4400. **b** Magnification $\times 40,000$. The bar represents 0.5 μm . **b** Magnification $\times 80,000$. The bar represents 0.2 μm

is essentially dispersed into the PA12 phase. It can be already seen in Fig. 1, but it is much more visible on Fig. 2, where the same sample and a second one at higher CB content (23.5 wt%) have been characterized using AFM (ScienTec, PicoLE, equipped with a conductive tip). On the amplitude image, the nodules of Pebax© are clearly identified. On the electrical image, the black spots correspond to the conductive filler. The comparison between the two images indicates that the CB is essentially dispersed in the PA12. Consequently, whatever the morphology of the dispersed Pebax©, it is the connectivity of the CB network through the continuous PA12 phase that

Fig. 2 AFM images of compounds with **a** 17 wt% CB and **b** 23.5 wt% CB (240 °C, 50 rpm, 4 min). *Left* Amplitude image and *right* electrical image



controls the conductivity of the material. To account for these facts, the CB content will be expressed in the following as function of the PA12 content only (it means the mass of CB divided by the mass of CB and PA12).

The type of CB used is Ensaco 250 (Timcal, Belgium). It is a powder of high structure (oil absorption number, 290 ml/100 g) and is easily dispersible. It has a BET surface area of 62 m²/g. CB quantity has been varied from 12 to 34% in weight on PA12 basis.

Mixing

All the CPC are prepared in an internal mixer Haake Rheomix 600P, with two counter-rotating rotors of the roller type. The protocol is as follows: First, the matrix components (PA12 and Pebax©) are introduced in the chamber. During 1 min, these components are melted and mixed. Then, the CB is added and mixed during a fixed time. The studied parameters are the rotation speed of the rotors, the regulation temperature of the chamber, and the mixing time. We have selected standard

conditions as 100 rpm, 240 °C, and 4 min. Beside these conditions, we have varied the rotor speed from 50 to 200 rpm, the temperature from 220 to 270 °C, and the mixing time from 2 to 10 min. At the end of the mixing time, samples are collected and compression molded as sheets of 100×50×2 mm, using an hydraulic press (240 °C, 10 MPa). These sheets are then used for electrical and rheological characterizations.

Resistivity measurements

Two stripes of conductive silver lake are deposited on each side of the compressed sheets. Measurements of electrical resistance r between these electrodes are conducted using a megohmmeter ISO Plus. Superficial resistivity is, thus, calculated as:

$$\rho_{\text{superficial}} = \frac{rL}{d} \quad (1)$$

where r is the resistance, d the distance between the electrodes, and L the length of the electrodes. For each

sample, at least two measurements are made. Depending on the CB content, the range of measured resistance varies from $10^{13} \Omega$ (isolating matrix) to $10^2 \Omega$ (perfectly conductive polymer).

Rheological measurements

Measurements are performed in oscillatory shear, using a parallel plate rheometer (Rheometrics RMS 800). Samples of 25-mm diameter are cut in the sheets used for resistance measurements using a punch. Before measurements, the samples are dried under vacuum during one night at 80°C .

All experiments are conducted at 240°C , under nitrogen to prevent degradation. To characterize the conductive network created by the percolation of CB, we follow a protocol already used for the evaluation of biscuit dough (Vergnes et al. 2003). At a constant frequency of 1 rad/s, we apply three successive strain sweeps, the first one from 0.5 to 100%, the second from 100 to 0.5%, and finally, the third, again, from 0.5 to 100%. The first strain sweep allows one to break the initial structure, the second to characterize the level of structure breakdown, and the third, after a fixed rest time, may allow the study of the eventual restoration of the structure. In the present study, rest time was always equal to zero.

In fact, instead of parallel plate geometry, it would have been more correct to use a cone and plate configuration to expose all the material to the same deformation. However, it is much easier to work with a parallel plate configuration, mainly for highly filled materials. As our intention is principally to compare the materials obtained in different processing conditions, this is not crucial in our opinion. Anyway, we have also performed an experiment in cone and plate configuration, and we will show later on that the results are similar.

Influence of mixing conditions on electrical properties

Percolation curves

For fixed mixing conditions, the percolation curve indicates the evolution of the superficial resistivity with CB content. As it can be seen in Fig. 3, a typical percolation curve is divided in three parts: At low CB content (less than 14 wt%), resistivity is constant and very high ($10^{12} \Omega$), and corresponds to the isolating properties of the polymer matrix. Between 14 and 30 wt%, resistivity drops rapidly over 11 decades. It is the percolation region, corresponding to the transition between isolating and conductive material. Finally, above 30 wt% CB, superficial resistivity is very low (less than 100Ω). It corresponds to the conductive plateau. For the targeted industrial application of these conductive

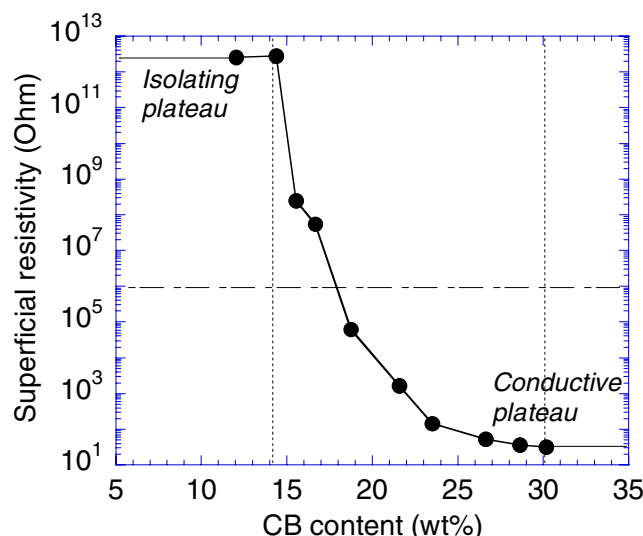


Fig. 3 Percolation curve (240°C , 100 rpm, 4 min)

polyamides, the required resistivity is less than $10^6 \Omega$. It can be seen in Fig. 3 that, for these processing conditions, the necessary CB content is around 18 wt%.

Influence of temperature

For a rotor speed of 100 rpm and a mixing time of 4 min, the regulation temperature has been set at 220, 240, and 270°C . Of course, the real-product temperature does not remain constant during mixing. Because of viscous heating, it increases regularly with time and reaches a stabilized value after 4 to 5 min. For the three selected regulation temperatures, the final product temperatures were, respectively, around 250, 265, and 290°C . Figure 4 shows that the corresponding percolation curves are very close. However, at fixed CB content, it appears that the conductivity is

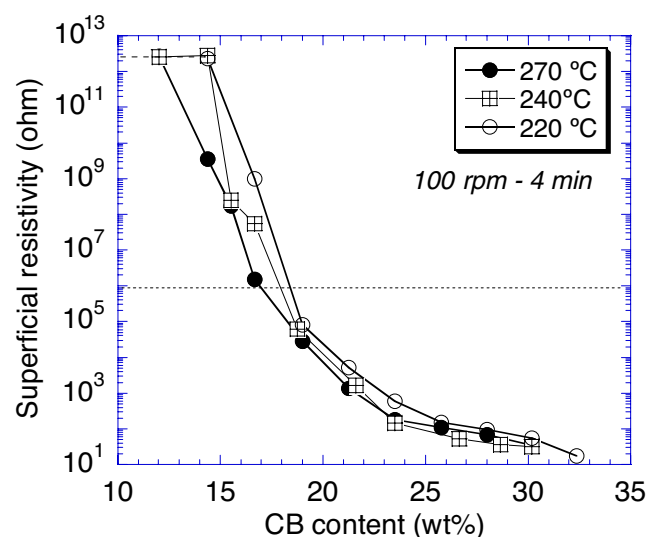


Fig. 4 Influence of regulation temperature on percolation curves (100 rpm, 4 min; temperature, 220, 240, and 270°C)

increased at higher temperature. It seems that a higher temperature during mixing is favorable to the formation of a conductive network, probably in relationship with a drop in matrix viscosity. Feller et al. (2002) observed a similar effect during the preparation of poly(butylene terephthalate)/poly(ethylene-co-ethyl acrylate) CPC on a twin screw extruder. Increasing processing temperature from 240 to 280 °C resulted in a decrease of resistivity, which was divided by approximately 2.5. In another paper, Feller and Petitjean (2003) confirmed these effects during single screw extrusion of a polybutylene terephthalate/Pebax® blend, filled with 16 wt% CB. By increasing the regulation temperature from 240 to 260 °C, they observed that the resistivity was divided by a factor 2. A drop of resistivity of elastomer/CB materials with an increase of regulation temperature was also noticed by Das et al. (2002) on an internal mixer and by Wan et al. (2005) on a two-roll mill. Yu et al. (1998) have also reported a decrease in resistivity with a decrease of matrix viscosity. All these results are contrary to the usual findings for the problems of dispersion of CB agglomerates, where a low temperature is usually favorable to dispersion because it increases the viscosity and, thus, the stresses capable to break the agglomerates (Manas-Zloczower et al. 1982; Rwei et al. 1991).

Influence of rotation speed

Figure 5 shows the percolation curves obtained at three different rotor speeds of 50, 100, and 200 rpm for a mixing time of 4 min and a temperature of 240 °C. We can see that the superficial resistivity decreases with the rotation speed: The value of $10^6 \Omega$ is reached for 17 wt% CB at 50 rpm and for 21 wt% CB at 200 rpm. These results seem to be contradictory with the preceding ones, as the viscosity

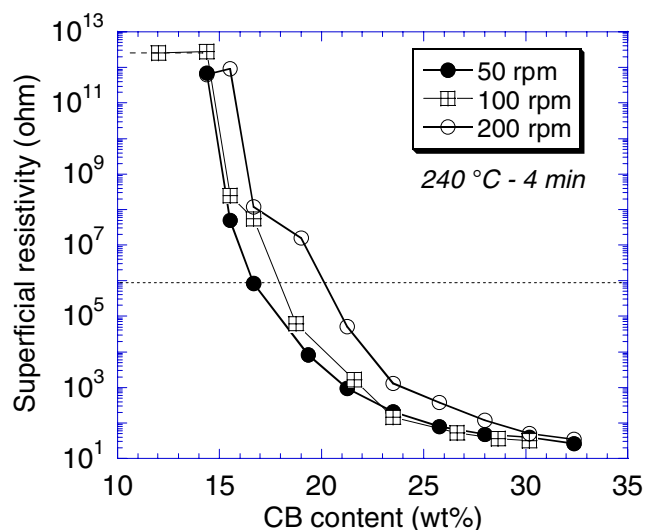


Fig. 5 Influence of rotors rotation speed on percolation curves (240 °C, 4 min; rotor speed, 50, 100, and 200 rpm)

tends to increase at low rotation speed because both viscous heating and shear rate are lower. Anyway, Das et al. (2002) have observed the same tendency during mixing of elastomers with CB on an internal mixer. They attributed this result to an increased breakup of the conductive structure at high speed. Feller and Petitjean (2003) and Wan et al. (2005) also reported an increase in resistivity when shear rate is increased.

These results clearly show that the formation of a conductive network implies mechanisms that are different from those involved in the simple dispersion of agglomerates. Indeed, as for the temperature, it is well known that an increase in rotor speed, thus, in shear rate, is favorable to the breakup and erosion mechanisms (Bohin et al. 1996; Scurati et al. 2002).

Influence of mixing time

Percolation curves for three different mixing times (2, 4, and 10 min) at 240 °C and 100 rpm are presented in Fig. 6. We can see that there is quite no difference for the short times (2 and 4 min). However, the longest time leads to higher resistivity for a fixed CB content. Once again, this result is at the opposite of the well-known effect of time in filler dispersion (Bohin et al. 1996; Scurati et al. 2002). However, in the case of resistivity, all the authors are unanimous to claim that the resistivity increases with the mixing time (Boonstra 1977; Cembrola 1983; Lee 1992; Yu et al. 1998; Das et al. 2002; Kalyon et al. 2002; Feller and Petitjean 2003; Wan et al. 2005). This is generally explained by a progressive deterioration of the network structure created during the first instants of the mixing process. When the dispersion is improved, the size of CB agglomerates diminishes, and the distance between them

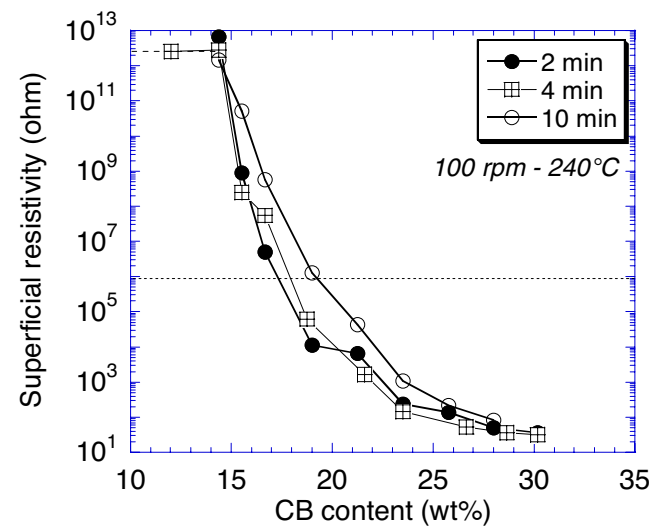


Fig. 6 Influence of mixing time on percolation curves (240 °C, 100 rpm; mixing time, 2, 4, and 10 min)

tends to increase, inducing the observed drop in electrical conductivity.

Summary on the influence of mixing conditions

If we compare the different results obtained by varying temperature, rotor speed, and mixing time, we observe that the changes in percolation curves are weak, even if they are real. For example, whatever the mixing conditions, the requested superficial resistivity of $10^6 \Omega$ is obtained for CB contents between 17 and 21 wt%. This is, perhaps, because of the limited range of processing conditions we tested. The best conditions appear to be 50 rpm/4 min/240 °C, 100 rpm/2 min/240 °C, and 100 rpm/4 min/270 °C, i.e., weak mixing conditions. This is in agreement with the findings of Pécastaigns (2005) who showed, using a modified AFM, a reduction of the conductive paths with increased mixing intensity. To summarize, the formation of a conductive network necessitates low shear rate, high temperature, and short time.

Rheological characterization

CPC with 19 wt% CB realized in standard mixing conditions (100 rpm, 4 min, 240 °C)

As explained in a previous section, the structure of the CPC is characterized through successive strain sweeps. In the following, we just present results concerning the storage modulus G' , as loss modulus G'' exhibits the same tendencies. In Fig. 7 are shown the results obtained with the two configurations, parallel plate (Fig. 7a), and cone and plate (Fig. 7b). We may observe that the global trends and the orders of magnitude are similar, what justifies for the following the use of the parallel plate configuration.

In Fig. 7a, the first strain sweep is characterized by a high initial modulus ($G' = 2.1 \cdot 10^4$ Pa) and a reduced linear domain ($\gamma_{lim} \approx 0.6\%$). As soon as the strain increases, storage modulus decreases to reach $5.4 \cdot 10^3$ Pa at 100% strain. For filled rubbers, this strain dependence is usually referred to as the Payne effect (Payne 1965). During the backwards strain sweep, we observe a large hysteresis, the modulus being always lower than during the first sweep. This could be explained by an evolution of the initial structure of the material (Vergnes et al. 2003). This assumption is confirmed by the fact that, during the third strain sweep, the linear domain has been largely increased ($\gamma_{lim} \approx 5\%$). Of course, for an unfilled system as the pure matrix, such experiments lead to superimposed curves for the successive strain sweeps. The hysteresis observed on the filled materials is without any doubt related to a structural evolution.

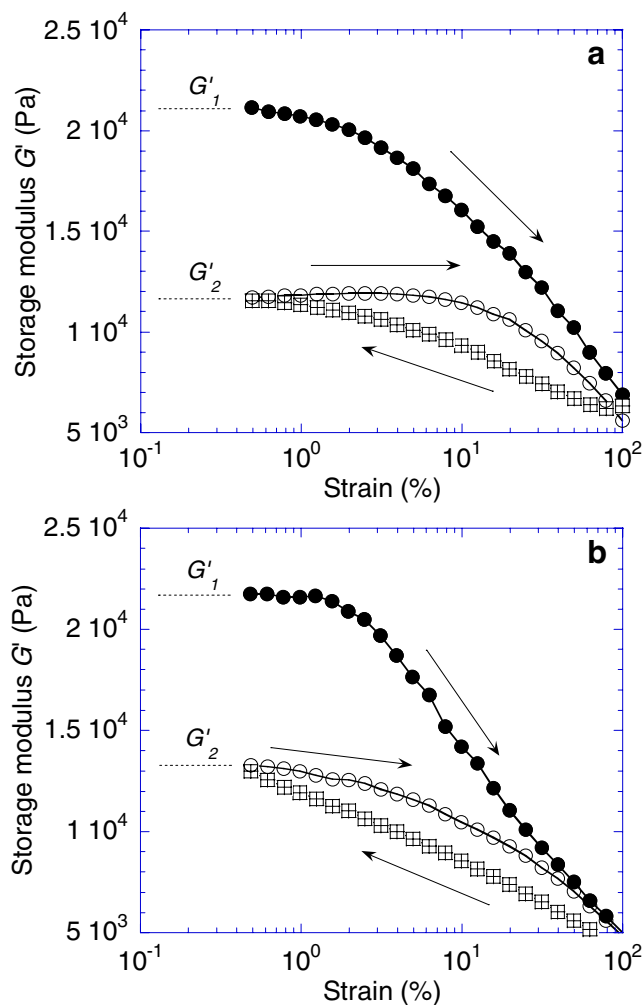


Fig. 7 Evolution of storage modulus G' during three successive strain sweeps at 1 rad s^{-1} for a CPC with 19 wt% CB (240 °C, 100 rpm, 4 min). **a** Parallel plate configuration, and **b** cone and plate configuration

We will use the values of the storage modulus in the linear domain of the first and third sweep, G'_1 and G'_3 , to characterize the CB network. We calculate the relative modulus drop by

$$\frac{\Delta G'}{G'} = \frac{G'_1 - G'_3}{G'_1} \quad (2)$$

Cassagnau and Mélis (2003) have performed successive strain sweeps on composites made of silica (16 wt%) and either polypropylene or polystyrene or EVA. They also observed a drop in moduli, followed by a long recovery (several hours) of the initial structure. In case of crystallization after the first strain sweep and subsequent melting, the recovery was total, indicating that the initial structure was created during the crystallization process and that this structure was kept in memory in the molten state, at least in the range of deformations studied (0.01–100%). Yurekli et al. (2001) have observed a fast (a few minutes) and total

recovery of the initial modulus after strain, but it was in the case of a maximum applied strain of 10%. In our case, we performed also a test with a fast cooling after the second sweep, followed by a melting and the third sweep. As it can be seen in Fig. 8, we observe only a partial recovery of the initial modulus, indicating that the deformations applied during the first sweep have implied some partially irreversible modifications of the initial CB structure.

CPC with 12 to 30 wt% CB realized in standard mixing conditions (100 rpm, 240 °C, 4 min)

In this section, we will consider a percolation curve obtained in standard mixing conditions (100 rpm, 240 °C, 4 min) and try to establish relationships between electrical and rheological properties.

First of all, we can see in Fig. 9 the global features of the rheological behavior of these composites according to the CB level. At low CB content (14 wt%), the behavior is controlled by the polymer matrix: The moduli are low ($G' = 10^4$ Pa), the linear domain is large ($\gamma_{lim} \approx 10\%$), and G'' is larger than G' on the whole domain of strain. When CB content increases (21 wt%), moduli increase ($G' = 3.1 \cdot 10^4$ Pa), linear domain decreases ($\gamma_{lim} \approx 1\%$), and the crossover of G' and G'' occurs around 2% strain. Finally, at high CB content (30 wt%), “solid” elastic behavior is dominant: Storage modulus is very large ($G' = 1.8 \cdot 10^5$ Pa), linear domain is largely reduced ($\gamma_{lim} < 0.5\%$), and the crossover of G' and G'' occurs at large deformation (30%). To summarize, when CB content increases along the percolation curve, the CPC behavior changes from the liquid viscous behavior of the matrix to an elastic solid behavior resulting from the structured CB network. The

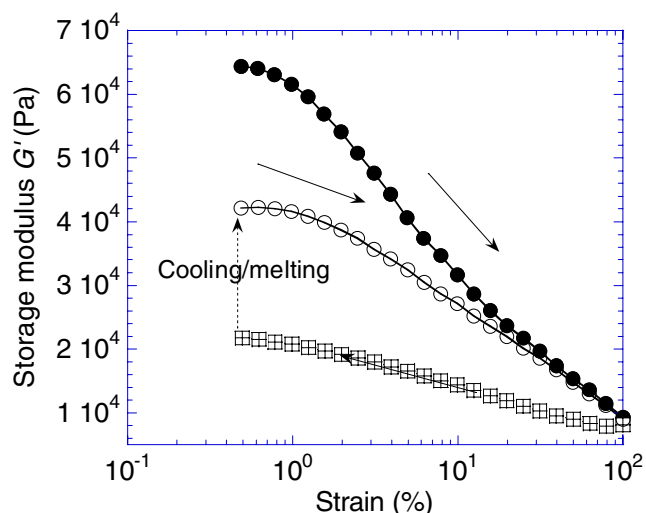


Fig. 8 Successive strain sweeps for a CPC with 23.5 wt% CB. A step of crystallization/melting has been included between the second and third sweep

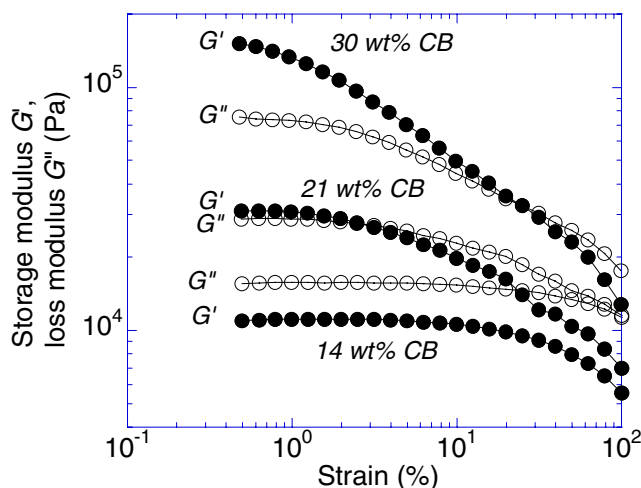


Fig. 9 Strain sweeps for CPC with 14, 21, and 30 wt% CB

variation in G' with CB content may appear limited, as compared to the corresponding variation in resistivity. But this rheological characterization has been made at 1 rad s^{-1} . The variations would be much higher at low frequency,

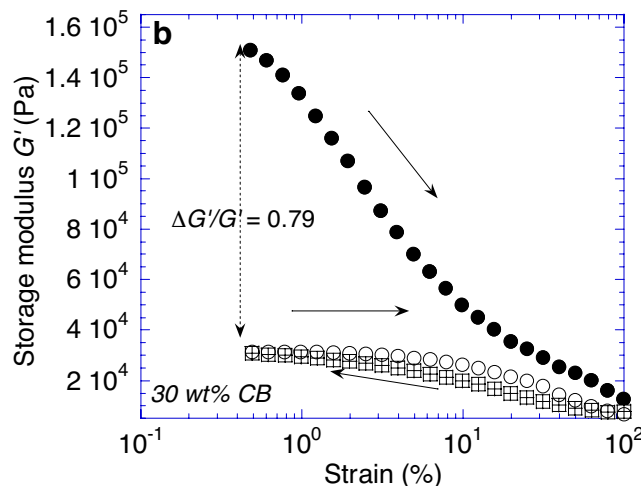
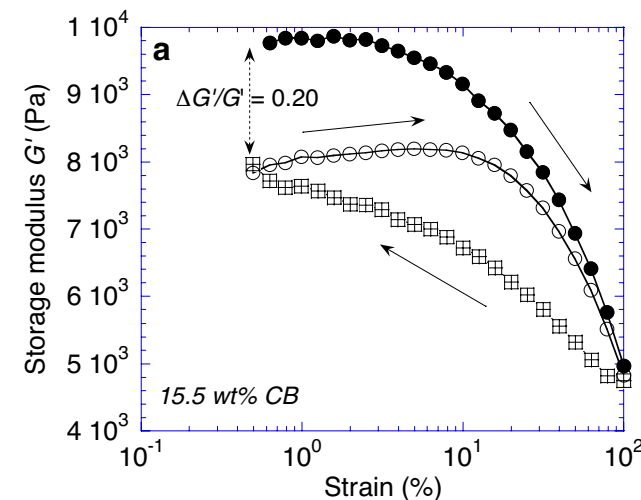


Fig. 10 Successive strain sweeps for CPC with **a** 15.5 wt% and **b** 30 wt% CB

0.01 rad s⁻¹, for example, as shown by Bar-Chaput and Carot (2006).

Figure 10 presents the strain sweeps for two CPC with, respectively, 15.5 and 30 wt% CB. As explained before, initial storage modulus and linear domain are largely affected by the CB content ($G' = 9.8 \cdot 10^3$ Pa, $\gamma_{lim} \approx 3\%$ at 15.5 wt% and $G' = 1.5 \cdot 10^5$ Pa, $\gamma_{lim} < 0.5\%$ at 30 wt%). But the most striking effect is the drop in storage modulus between the first and third strain sweeps: $\Delta G'/G'$ (Eq. 2) increases from 20 to 79% when CB content changes from 15.5 to 30 wt%. The level of structure breakdown induced by the deformation seems, thus, related to the initial structure of the network. It is clear that the linear domain is a function of the CB content, as shown, for example, by Yurekli et al. (2001). But the structure of the network is also implied. If we consider samples prepared in different mixing conditions and with different CB contents (respectively, 50 rpm, 4 min, 240 °C, and 17 wt% CB; 100 rpm, 10 min, 240 °C, and 19 wt% CB) but with the same superficial resistivity (1 MΩ), we observe in Fig. 11 that the linear domains are equivalent. This confirms that the electrical properties of the CPC are directly connected with the structure of the dispersed CB phase, which can be evaluated by rheological measurements.

Figure 12 shows the evolution of both superficial resistivity and relative modulus drop ($\Delta G'/G'$) with the CB content. We can see that the curves are symmetric, with three distinct zones. For CB values less than 14 wt%, $\Delta G'/G'$ is almost constant and close to zero when resistivity is also constant and maximum (10^{13} Ω). This zone corresponds to the isolating plateau, and the behavior is the one of the matrix. Then, for CB content between 14 and 27 wt%, resistivity decreases by 11 decades when $\Delta G'/G'$ increases from 5 to 80%. Finally, above 27 wt% CB, both

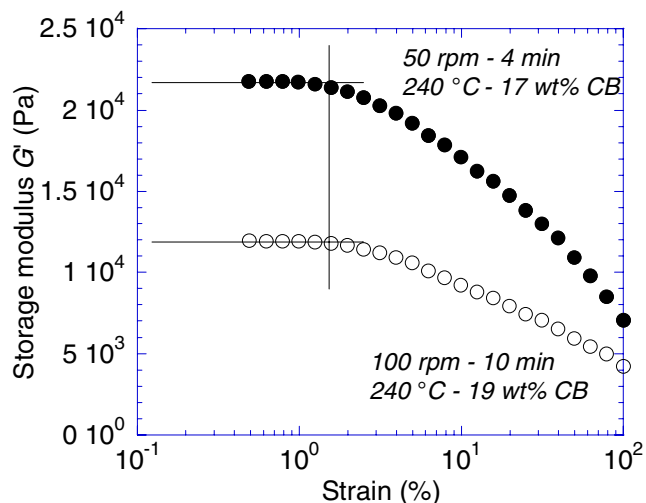


Fig. 11 Linear domains of two CPC with same resistivity (1 MΩ) mixed under different conditions with different CB contents

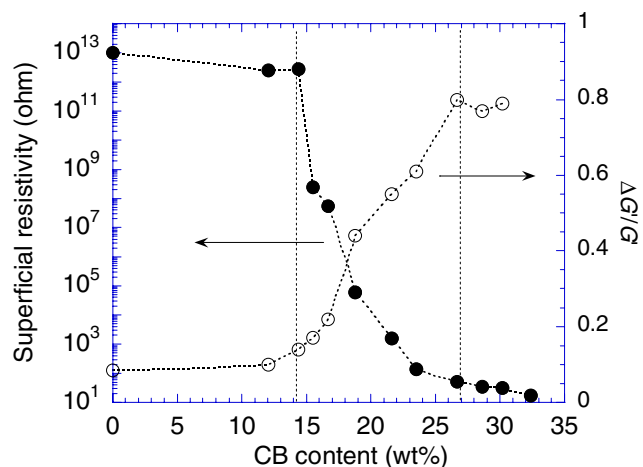


Fig. 12 Superficial resistivity and relative modulus drop $\Delta G'/G'$ as function of CB content

resistivity and $\Delta G'/G'$ are constant, what corresponds to the conductive plateau. It seems, thus, that resistivity and $\Delta G'/G'$ could be closely connected. It is confirmed in Fig. 13 where $\Delta G'/G'$ is plotted as a function of resistivity. The relationship between superficial resistivity and $\Delta G'/G'$ can be nicely expressed by a power law:

$$\frac{\Delta G'}{G'} = a \rho_{superficial}^b \tag{3}$$

where a and b are constants, depending eventually on the network structure. In the present case, $a = 0.956$ and $b = -0.071$.

To confirm the link between modulus drop and resistivity, we have performed specific experiments where rheological tests and resistivity measurements are conducted simultaneously. This work will be presented in details in a future paper, and we will just show in this paper an example of the results. On Fig. 14, it can be seen that, when

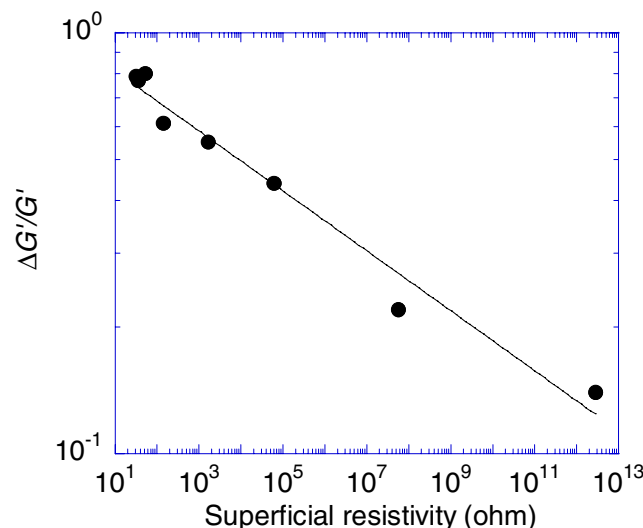


Fig. 13 Evolution of relative modulus drop $\Delta G'/G'$ with superficial resistivity

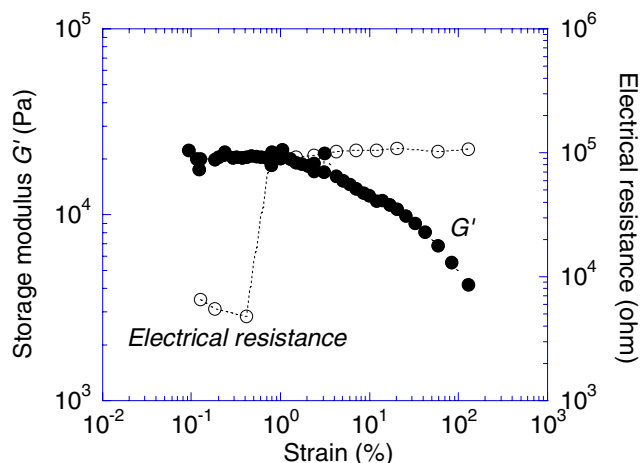


Fig. 14 Simultaneous measurement of the evolution of storage modulus G' and electrical resistance with the strain (22% CB, 100 rpm, 240 °C, 4 min)

the modulus starts to decrease above a certain strain, the electrical resistance jumps rapidly, indicating clearly a breakup of the conductive network.

Another way to represent the link between rheological and electrical data consists in plotting the storage modulus after deformation, G'_2 , as a function of its initial value, G'_1 , for different CB contents. As shown in Fig. 15, we obtain two connected straight lines. The first one, which corresponds to CB contents less than 15–17 wt%, has a slope nearly equal to one. It means that there is no change in storage modulus because of deformation. This part of the graph corresponds to the isolating plateau, where the rheological behavior is imposed by the matrix. Around 15–17 wt%, which corresponds to the percolation threshold, we observe a change in the slope. Above this point, G'_2 remains proportional to G'_1 but with a slope lower than 1. Now, we are facing a structured material whose structure is more or

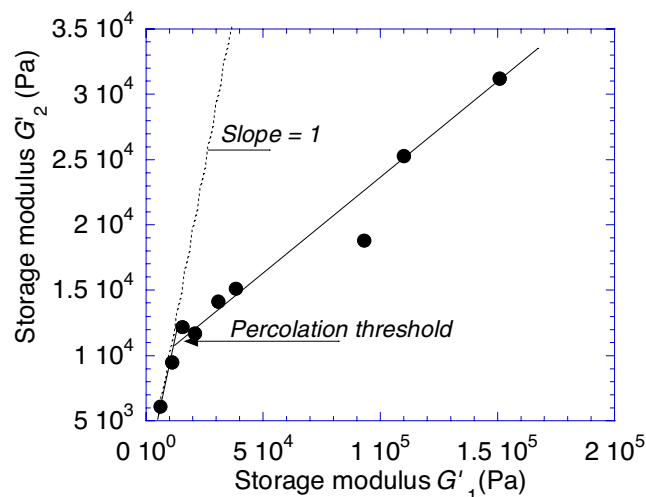


Fig. 15 Evolution of G'_2 as function of G'_1 for products with 12 to 30 wt% CB mixed in standard conditions (100 rpm, 240 °C, 4 min)

less destroyed by the imposed deformation. We can, then, assume that the deviation of this second line from the first one gives an idea of the strength of the structured network.

All these results show clearly that the electrical properties of the CPC are depending on the percolated structure developed during the mixing process and that these properties can be estimated through adapted rheological measurements.

Influence of mixing conditions

In Fig. 16, we are considering the effect of rotor speed on the properties of the CPC. Figure 16a shows the evolution of $\Delta G'/G'$ as function of CB content for three different rotor speeds. We can see that the different curves are overlapping without any clear tendency. On the opposite, if we consider the same data but presented as G'_2 as a function of G'_1 (Fig. 16b), we can nicely rank the different speeds according to the slopes of the second part of the lines. In

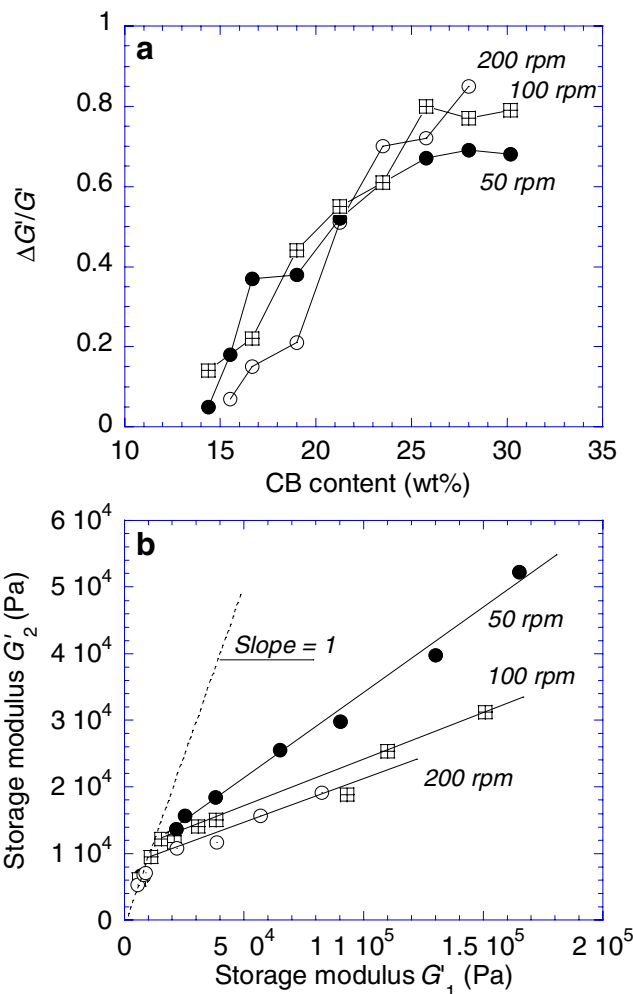


Fig. 16 Influence of rotor speed (240 °C, 4 min; 50, 100, and 200 rpm). **a** Evolution of relative modulus drop $\Delta G'/G'$ with CB content; **b** evolution of G'_2 as a function of G'_1

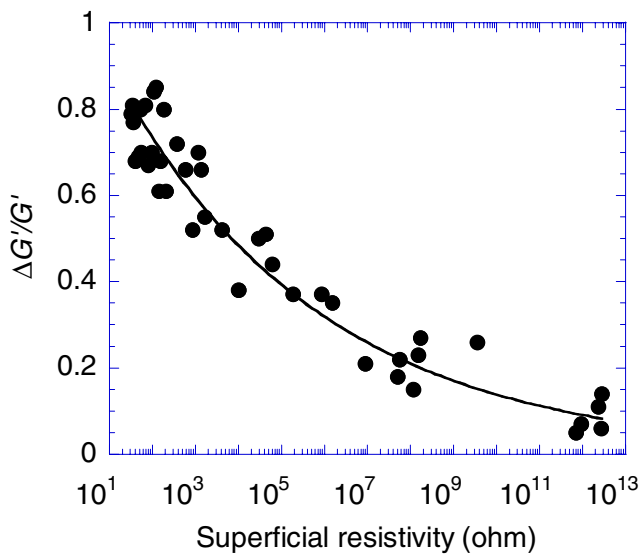


Fig. 17 Evolution of relative modulus drop $\Delta G'/G'$ with superficial resistivity for all the experimental conditions. The line represents the fit by a power law

this case, 50 rpm appears as the most favorable condition followed by 100 and 200 rpm. This ranking corresponds to the one established according to the percolation curves (see Fig. 5). It has been shown with the different conditions tested that the G'_2 vs G'_1 representation was always the most representative. Therefore, only these graphs will be presented in the following. However, the relationship between $\Delta G'/G'$ and electrical resistivity put in evidence in Fig. 13 remains valid, more or less independently of the mixing conditions. It can be seen in Fig. 17 that a power law relationship can be established for the whole experimental points. The superficial resistivity of the CPC can be estimated from rheological measurements by Eq. 3, with the following values of parameters: $a=1.1132$ and $b=-0.09$.

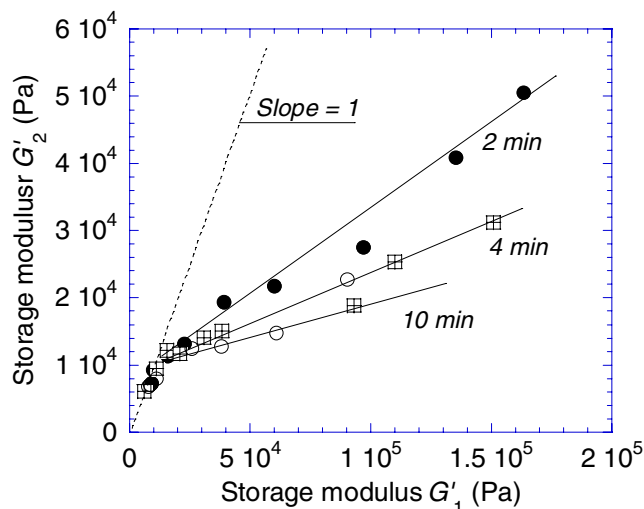


Fig. 18 Evolution of G'_2 as function of G'_1 for different mixing times (2, 4, and 10 min)

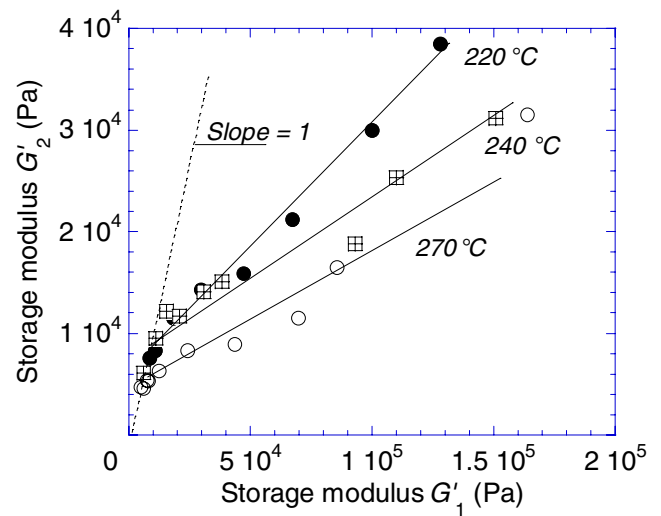


Fig. 19 Evolution of G'_2 as function of G'_1 for different regulation temperatures (220, 240, and 270 °C)

The influences of the mixing time and the regulation temperature are shown in Figs. 18 and 19. For the mixing time, the ranking obtained from the rheological curves is the same as the one deduced from the percolation curves (Fig. 6). However, for the temperature, we obtain an opposite result, the best condition being 220 °C according to the rheology and 270 °C according to the percolation curve. We may imagine that the high temperatures could have led to a thermal degradation of the matrix. To clarify this point, we have performed measurements of viscosity in solution for different samples at 17 wt% CB. For samples prepared in gentle conditions (240 °C, 4 min, and 50 rpm; 240 °C, 2 min, and 100 rpm), the viscosity is equal to 1.80 ± 0.02 . It decreases to 1.72 when speed is increased to 200 rpm (240 °C, 4 min), to 1.64 when mixing time is increased to 10 min (240 °C, 100 rpm), and finally to 1.61 when

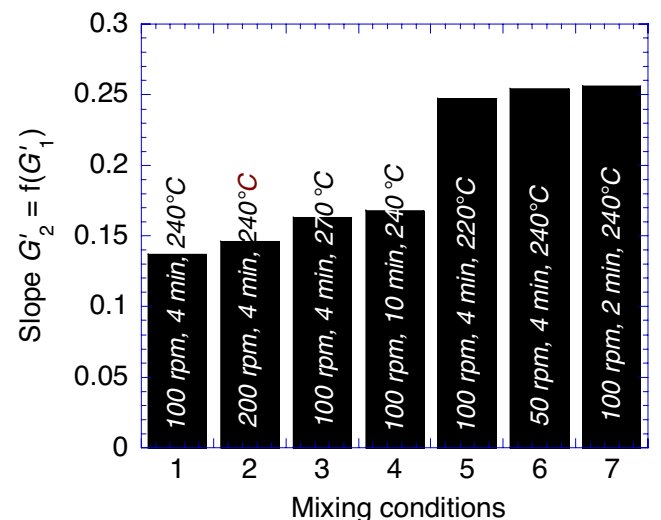


Fig. 20 Slope of G'_2 vs G'_1 for different mixing conditions

temperature is increased to 270 °C (4 min, 100 rpm). We observe, thus, a decrease in molecular weight induced by thermomechanical degradation for the samples prepared in strong mixing conditions. However, this effect cannot explain easily the influence of temperature seen before.

To summarize, we have indicated in Fig. 20 the values of the slope of the G'_2 vs G'_1 curves for the different mixing conditions. The higher the slope, the better are the mixing conditions. It confirms that, for obtaining a strong conductive network, low rotor speed and short mixing time are preferable. As explained before, the exact role of the temperature remains ambiguous.

Conclusion

We have characterized the electrical resistivity of CPC obtained by mixing CB with a PA12/Pebax© matrix. In a first part, we have shown that the percolation curves were modified by the mixing conditions. The best conductive properties were obtained at low rotor speed, high temperature, and short mixing time, indicating that the conditions leading to the formation of a conductive network were different from those necessary for a good filler dispersion. In a second part, we have carried out successive strain sweeps on these CPC to characterize the structure of the network. We have shown that, depending on CB content, different behaviors could be observed, ranging from the fluid behavior of the matrix to a solid-like elastic behavior. The existing initial structure is modified by the imposed strain in a way which seems partially irreversible. By measuring the storage modulus in the linear domain before and after strain, it is possible to establish clear relationships between electrical properties and rheological responses. To put in evidence the influence of the mixing parameters on the “strength” of the conductive network, we propose to plot the storage modulus after deformation, G'_2 , as a function of its initial value, G'_1 , for different CB contents.

References

Bar-Chaput S, Carrot C (2006) Rheology as a tool for the analysis of the dispersion of carbon filler in polymers. *Rheol Acta* 45:339–347

Bohin F, Manas-Zloczower I, Feki DL (1996) Kinetics of dispersion for sparse agglomerates in simple flows: application to silica agglomerates in silicone polymers. *Chem Eng Sci* 51:5193–5204

Boonstra BB (1977) Resistivity of unvulcanized compounds of rubber and carbon black. *Rubber Chem Technol* 50:194–210

Boonstra BB, Medalia IA (1963) Effect of carbon black dispersion on the mechanical properties of rubber vulcanizates. *Rubber Chem Technol* 36:115–142

Carmona F, Ravier J (2002) Electrical properties and mesostructure of carbon black-filled polymers. *Carbon* 40:151–156

Cassagnau P, Méliis F (2003) Non-linear viscoelastic behaviour and modulus recovery in silica filled polymer. *Polymer* 44:6607–6615

Cembrala RJ (1983) Resistivity and surface roughness analysis for evaluating carbon black dispersion in rubber. *Rubber Chem Technol* 56:233–245

Das NC, Chaki TK, Khashtgir D (2002) Effect of processing parameters, applied pressure and temperature on the electrical resistivity of rubber-based conductive composites. *Carbon* 40:807–816

Feller JF, Petitjean E (2003) Conductive polymer composites (CPC): influence of processing conditions, shear rates and temperatures on electrical properties of poly(butylene terephthalate)/poly(amide12-*b*-tetramethyle-neglycol)-carbon black blends. *Macromol Symp* 203:309–315

Feller JF, Linossier I, Charpentier A (2002) Conductive polymer composites (CPC): influence of processing conditions, shear rate and temperature, on electrical properties of poly(butylenes terephthalate)/poly(ethylene-co-ethyl acrylate)-carbon black blends. *Proceedings of the 19th Congress of the Polymer Processing Society, Guimaraes, CD ROM*

Kalyon DM, Birinci E, Yazici R, Karuv B, Walsh S (2002) Electrical properties of composites as affected by the degree of mixedness of the conductive filler in the polymer matrix. *Polym Eng Sci* 42:1609–1617

Kohjiya S, Katoh A, Shimanuki J, Hasegawa T, Ikeda Y (2005) Nanostructural observation of carbon black dispersion in natural rubber matrix by three dimensional transmission electron microscopy. *J Mater Sci* 40:2553–2555

Kohjiya S, Katoh A, Suda T, Shimanuki J, Ikeda Y (2006) Visualisation of carbon black networks in rubbery matrix by skeletonisation of 3D-TEM image. *Polymer* 47:3298–3301

Lee BL (1992) Electrically conductive polymer composites and blends. *Polym Eng Sci* 32:36–42

Lux F (1993a) Models proposed to explain the electrical conductivity of mixtures made of conductive and insulating materials. *J Mater Sci* 28:285–301

Lux F (1993b) Percolation in electrical conductive polymer/filler systems. I. Density/filler curves according to a new thermodynamic percolation model. *Polym Eng Sci* 33:334–342

Manas-Zloczower I, Nir A, Tadmor Z (1982) Dispersive mixing in internal mixers. A theoretical model based on agglomerate rupture. *Rubber Chem Technol* 55:1250–1285

Margolis JM (1989) *Conductive polymers and plastics*. Chapman & Hall, New York

Medalia AI (1986) Electrical conduction in carbon black composites. *Rubber Chem Technol* 59:432–454

Meincke O, Kaempfer D, Weickmann H, Friedrich C, Vathauer M, Warth H (2004) Mechanical properties and electrical conductivity of carbon-nanotube filled polyamide-6 and its blends with acrylonitrile/butadiene/styrene. *Polymer* 45:739–748

Payne AR (1965) *Reinforcement of elastomers*. Interscience, New York

Pécastaigns G (2005) Contribution à l'étude et à la modélisation de la mésostructure de composites polymères-noir de carbone. Thèse de Doctorat, Université Bordeaux

Pötschke P, Bhattacharyya AR, Janke A (2003) Morphology and electrical resistivity of melt mixed blends of polyethylene and carbon nanotube filled polycarbonate. *Polymer* 44:8061–8069

Pötschke P, Bhattacharyya AR, Janke A (2004) Carbon nanotube-filled polycarbonate composites produced by melt mixing and their use in blends with polyethylene. *Carbon* 42:965–969

Ravier J, Houzé F, Carmona F, Schneegans O, Saadaoui H (2001) Mesostructure of polymer/carbon black composites observed by conductive probe atomic force microscopy. *Carbon* 39:287–324

Rwei SP, Feki DL, Manas-Zloczower I (1991) Characterization of agglomerate dispersion by erosion in simple shear flow. *Polym Eng Sci* 31:558–562

- Scurati A, Feke DL, Manas-Zloczower I (2002) Model and analysis for kinetics of agglomerate erosion in simple shear flows. Meeting of the ACS Rubber Division, Savannah, Georgia
- Sichel EK (1982) Carbon black—polymer composites. Marcel Dekker, New York
- Thongruang W, Spontak RJ, Balik CM (2002) Bridged double percolation in conductive polymer composites: an electrical conductivity, morphology and mechanical property study. *Polymer* 43:3717–3725
- Vergnes B, Della Valle G, Colonna P (2003) Rheological properties of biopolymers and applications to cereal processing. In: Galetunk G, Breslauer KJ (eds) *Characterization of cereals and flours*. Marcel Dekker, New York, pp 209–265
- Wan Y, Xiong C, Yu J, Wen D (2005) Effect of processing parameters on electrical resistivity and thermo-sensitive properties of carbon-black/styrene-butadiene-rubber composite membranes. *Compos Sci Technol* 65:1769–1779
- Wu G, Zheng Q (2004) Estimation of the agglomeration structure for conductive particles and fiber-filled high-density polyethylene through dynamic rheological measurements. *J Polym Sci B Polym Phys* 42:1199–1205
- Wu G, Asai S, Sumita M, Hattori T, Higuchi R, Washiyama J (2000) Estimation of flocculation structure in filled polymer composites by dynamic rheological measurements. *Colloid Polym Sci* 278:220–228
- Wu G, Lin J, Zheng Q, Zhang M (2006) Correlation between percolation behavior of electricity and viscoelasticity for graphite filled high density polyethylene. *Polymer* 47:2442–2447
- Yu G, Zhang MQ, Zeng HM (1998) Carbon black filled polyolefine as a positive temperature coefficient material: effect of composition, processing and filler treatment. *J Appl Polym Sci* 70:559–566
- Yu J, Zhang LQ, Rogunova M, Summers J, Hiltner A, Baer E (2005) Conductivity of polyolefins filled with high-structure carbon black. *J Appl Polym Sci* 98:1799–1805
- Yui H, Wu G, Sano H, Sumita M, Kino K (2006) Morphology and electrical conductivity of injection-molded polypropylene/carbon black composites with addition of high-density polyethylene. *Polymer* 47:3599–3608
- Yurekli K, Krishnamoorti R, Tse MF, McElrath KO, Tsou AH, Wang HC (2001) Structure and dynamics of carbon black-filled elastomers. *J Polym Sci B Polym Phys* 39:256–275